

1           **Physicochemical study of mixed systems composed by bovine caseinate and the**  
2                           **galactomannan from *Gleditsia amorphoides***

3    Débora N. López<sup>a</sup>, Micaela Galante<sup>a</sup>, Estela M. Alvarez<sup>a</sup>, Patricia H. Risso<sup>a,b,c</sup>, Valeria Boeris<sup>a,d\*</sup>

4    <sup>a</sup> Departamento de Química-Física, Facultad de Ciencias Bioquímicas y Farmacéuticas,  
5    Universidad Nacional de Rosario (UNR) – CONICET. Suipacha 531, Rosario, Argentina.

6    <sup>b</sup> Facultad de Ciencias Veterinarias, UNR, Ovidio Lagos y Ruta 33, Casilda, Argentina.

7    <sup>c</sup> Instituto de Física Rosario (IFIR, CONICET-UNR), 27 de Febrero 210 Bis, Rosario, Argentina

8    <sup>d</sup> Facultad de Química e Ingeniería del Rosario, Pontificia Universidad Católica Argentina.  
9    Pellegrini 3314, Rosario, Argentina

10  
11   **\*Corresponding Author:**

12    Dra. Valeria Boeris

13    Facultad de Ciencias Bioquímicas y Farmacéuticas. Universidad Nacional de Rosario - CONICET  
14    Suipacha 531. (S2002RLK) Rosario. Argentina.

15    e-mail: [valeriaboeris@conicet.gov.ar](mailto:valeriaboeris@conicet.gov.ar)

16

17 **Abstract**

18 Model systems formed by sodium caseinate (NaCAS) and espina corona gum (ECG) were  
19 studied. There was no evidence of attractive interactions between NaCAS and ECG  
20 macromolecules. Aqueous mixtures of NaCAS and ECG phase-separate segregatively over a wide  
21 range of concentrations. According to the images obtained by confocal laser scanning microscopy,  
22 NaCAS particles form larger protein aggregates when ECG is present in the system. An increase  
23 in the hydrodynamic diameter of NaCAS particles, as a result of ECG addition, was also observed  
24 by light scattering in diluted systems. A depletion-flocculation phenomenon, in which ECG is  
25 excluded from NaCAS surface, is proposed to occur in the concentrated mixed systems, resulting  
26 in NaCAS aggregation. ECG raises the viscosity of NaCAS dispersions without affecting the  
27 Newtonian flow behaviour of NaCAS. These results contribute to improve the knowledge of a  
28 barely-studied hydrocolloid which may be useful in the development of innovative food systems.

29 **Keywords:** sodium caseinate, espina corona gum, biopolymer interaction, food systems

30

31

## 32 **1. Introduction**

33 Protein-polysaccharide mixtures are widely used in the food industry in order to impart  
34 desirable texture and sensory characteristics (Dickinson, 1998; Mohajer, Rezaei, & Hosseini).  
35 Understanding the behaviour of the systems composed either by milk proteins or hydrocolloids is  
36 of great importance, since the functional properties of milk proteins are usually affected by  
37 polysaccharides (Matignon et al., 2014; Mende et al., 2013; Rosa-Sibakov et al., 2016).

38 Due to their physicochemical and functional properties, sodium caseinates (NaCAS) are  
39 useful ingredients added to different food products as emulsifiers, gelling, texturizing and water  
40 and fat binding agents (Gaucheron, Le Graet, Boyaval, & Piot, 1997; Perrechil, Braga, & Cunha,  
41 2009).

42 Vegetable galactomannans are a group of environment-friendly polysaccharides obtained  
43 from seeds of some Leguminosae tree and consist of chains of mannose residues with randomly  
44 attached galactose units as side-chains (Tavares, Monteiro, Moreno, & Da Silva, 2005). Many plant  
45 gums (e.g. carrageenan, pectin, starch, guar and sodium carboxyl methyl cellulose) are broadly  
46 used in food systems as thickeners, gelling and suspending agents, texture modifiers, emulsifiers  
47 and emulsion stabilizers (Balaghi, Mohammadifar, & Zargaraan, 2010; Dickinson, 1989; Saha &  
48 Bhattacharya, 2010). Mixed systems composed of food proteins and many galactomannans like  
49 guar gum, locust bean gum and tara gum, among others, have been extensively studied (Tavares &  
50 Da Silva, 2003).

51 Espina corona gum (ECG), the polysaccharide used in this work, is a galactomannan  
52 extracted from the seeds of *Gleditsia amorphoides*, a leguminous tree (Pavón, Lazzaroni, Sabbag,  
53 & Rozycki, 2014) and its chemical composition was described by Cerezo in 1965 (Cerezo, 1965).  
54 The molecular weight of ECG is 1390 Da and the galactose/manose ratio in ECG is 2.5 (Perduca  
55 et al., 2013) , similar to that of guar gum, one of the galactomananns of the utmost commercial

56 importance. It is a non-gelling biopolymer that may be used as a food thickener or stabilizer. In  
57 fact, the mechanical and microstructural properties of milk whey protein/ECG mixed gels were  
58 studied (Spotti, Santiago, Rubiolo, & Carrara, 2012) and a recent investigation reported the  
59 addition of ECG in cholesterol-reduced probiotic yoghurts (Pavón et al., 2014). However, the  
60 applications of this galactomannan have not yet been well studied (Albuquerque et al., 2014) and  
61 its effects on aqueous suspensions of NaCAS have not been reported so far.

62 The aim of this work was to study, from a physicochemical point of view, a model system  
63 containing NaCAS and ECG in order to explore future applications of this galactomannan in food  
64 products.

## 65 **2. Materials and Methods**

### 66 **2.1. Materials**

67 Bovine sodium caseinate (NaCAS) and 1-anilino-8-naphtalene-sulfonate (ANS) were  
68 purchased from Sigma-Aldrich (Steinheim, Germany). ECG was gently donated by Idea Supply  
69 Argentina S.A. (Chaco, Argentina), and was used without further purification.

### 70 **2.2. Preparation of the stock solutions**

71 NaCAS powder was dissolved in distilled water in order to obtain a 10 wt. % NaCAS  
72 solution. A 1 wt. % ECG stock solution was prepared by dispersing ECG powder in distilled water  
73 at room temperature and was kept in stirring until complete solubilization of the polysaccharide.  
74 Diluted systems were prepared for spectroscopic techniques to ensure the correct dissolution of  
75 both biopolymers and to avoid an inner filter effect. A 1 % w/v NaCAS and a 0.5 % w/v ECG stock  
76 solutions were prepared. A small amount of sodium azide, purchased from Mallinckrodt Chemical,  
77 (St. Louis, USA) was added to protein and polysaccharide suspensions in order to inhibit microbial  
78 development.

### 79 **2.3. Fluorescence spectroscopy**

### 80 **2.3.1. Intrinsic fluorescence spectra**

81 Fluorescence emission spectra of NaCAS (0.01 % w/v) were obtained at 35 °C, exciting at  
82 280 nm, at increasing concentrations of ECG (0-0.3 % w/v). The scanning rate was 10 nm/min and  
83 data acquisition was performed every 0.1 nm with a 0.1 nm slit from 300 to 400 nm in an Amico  
84 Browman spectrofluorometer Series 2000 using a thermostated quartz cell of 1 cm path length.  
85 The inner filter effect, caused by the absorption of the incident light or the emitted light, was  
86 corrected in all fluorescence intensity (FI) measurements (Lakowicz, 2007).

### 87 **2.3.2. Quenching of the intrinsic fluorescence**

88 The fluorescence quenching of NaCAS tryptophan residues, when excited at 280 nm, was  
89 carried out using 4 M acrylamide, which is a collisional quencher. Protein concentration was fixed  
90 at 0.01 % w/v, while ECG concentration ranged from 0 to 0.3 % w/v. Emission intensities were  
91 recorded at 340 nm in the absence of acrylamide (FI<sub>0</sub>) and after the addition of successive aliquots  
92 of 10 µL of quencher solution (FI).

### 93 **2.3.3. Surface hydrophobicity**

94 Surface hydrophobicity (S<sub>0</sub>) was estimated according to the method described by Kato and  
95 Nakai (Kato & Nakai, 1980), using the ammonium salt of the fluorescent probe 1-anilino-8-  
96 naphthalene-sulfonate (ANS). FI of samples containing 4 mM ANS and different concentrations of  
97 ECG/NaCAS mixtures were determined. Measurements were carried out at 35 °C using the  
98 excitation and emission wavelength set at 380 and 484 nm, respectively. The initial slope of FI vs.  
99 protein concentration plot was used to estimate NaCAS surface hydrophobicity.

### 100 **2.4. Zeta potential and hydrodynamic diameter measurements**

101 Zeta potential and the hydrodynamic diameter (HD) of NaCAS were determined at 35 °C  
102 in a Nano Particle Analyzer Horiba SZ-100. Protein concentration was fixed at 0.01 % w/v whereas  
103 ECG concentration varied over the range of 0-0.03 % w/v. Each solution was filtered through a

104 glass microfiber paper with a cut-off of 1.6  $\mu\text{m}$ , in order to avoid powders in suspensions. Such  
105 diluted systems were prepared in order to avoid interferences with the dynamic light scattering  
106 technique (Anema & Klostermeyer, 1996).

## 107 **2.5. Confocal scanning laser microscopy**

108 Immediately after mixing and after a 24-h incubation at 35 °C, the effect of ECG on 3%  
109 NaCAS dispersions was observed using confocal scanning laser microscopy (CSLM). Rhodamine  
110 B (Sigma-Aldrich, St. Louis, USA) was added to those systems at a final concentration of 0.1 mg  
111  $\text{L}^{-1}$ . Each sample (100  $\mu\text{L}$ ) was placed in a compartment of LAB-TEK II cells. Representative  
112 images were captured using a confocal microscopy (Nikon Eclipse TE-2000-E, Japan), with an  
113 objective of 60X (oil immersion lens), a magnification of 5X and a numerical aperture of 1.4.  
114 Digital images were acquired with a pixel resolution of 1024 X 1024.

## 115 **2.6. Evaluation of the biopolymer concentration ranges for phase separation**

116 Samples were prepared by carefully mixing weighed amounts of ECG and NaCAS stock  
117 solutions in order to obtain systems with different biopolymer composition (NaCAS and ECG  
118 concentrations ranged from 1 to 9 wt. % and between 0.1 and 0.9 wt. %, respectively). The systems  
119 were mixed in vortex and were placed under controlled temperature at 35 °C. The occurrence of  
120 phase separation was verified after 24 h of incubation, according to Hidalgo et al. (Hidalgo et al.,  
121 2015).

## 122 **2.7. Viscosity measurement**

123 The rheological measurements of NaCAS, NaCAS/ECG and ECG systems were performed  
124 at 35 °C using a viscometer Brookfield LVDV-II<sup>+</sup>CP (USA) in steady shear with a cone-plate  
125 geometry (diameter 48 mm, angle 0.8°).

## 126 **2.8. Statistical analysis**

127           The determinations were made at least in triplicate. The significance of the effect of ECG  
128 on each parameter was determined by means of t-test.

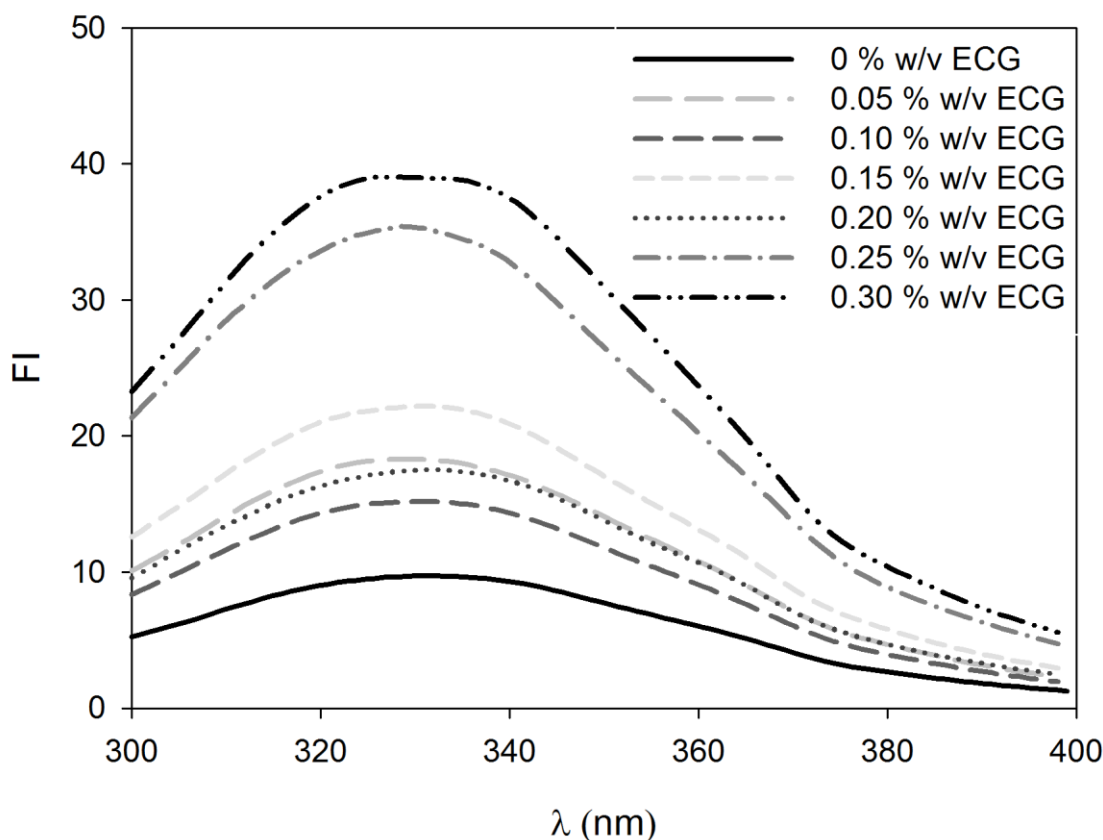
### 129 **3. Results**

#### 130 **3.1. Spectroscopic studies of the NaCAS/ECG diluted mixed systems**

131           Fluorimetric techniques allow the assessment of the global structure of proteins and  
132 therefore to determine the effect of ECG on NaCAS conformation in solution.

##### 133 **3.1.1. Intrinsic fluorescence spectra**

134           The emission spectra of NaCAS at increasing ECG concentrations are shown in Fig. 1. It is  
135 to be noted that Trp fluorescence contributes the most to protein spectra due not only to its higher  
136 quantum yield but also to the energy transfer from Phe to Tyr and from Tyr to Trp. The FI is usually  
137 related to the solvent exposition of this fluorescent aminoacid. There was a progressive increase in  
138 the FI values as the ECG concentration increased. On the other hand, maximum emission  
139 wavelength of the intrinsic fluorescence spectrum has been recurrently related to the  
140 hydrophobicity of the Trp microenvironment. Changes in the wavelength corresponding to the  
141 emission peak were not observed.



142  
 143 Fig. 1: Effect of ECG (0-0.3 % w/v) on the fluorescence emission spectra of NaCAS (0.01 % w/v)

144 **3.1.2. Quenching of the intrinsic fluorescence**

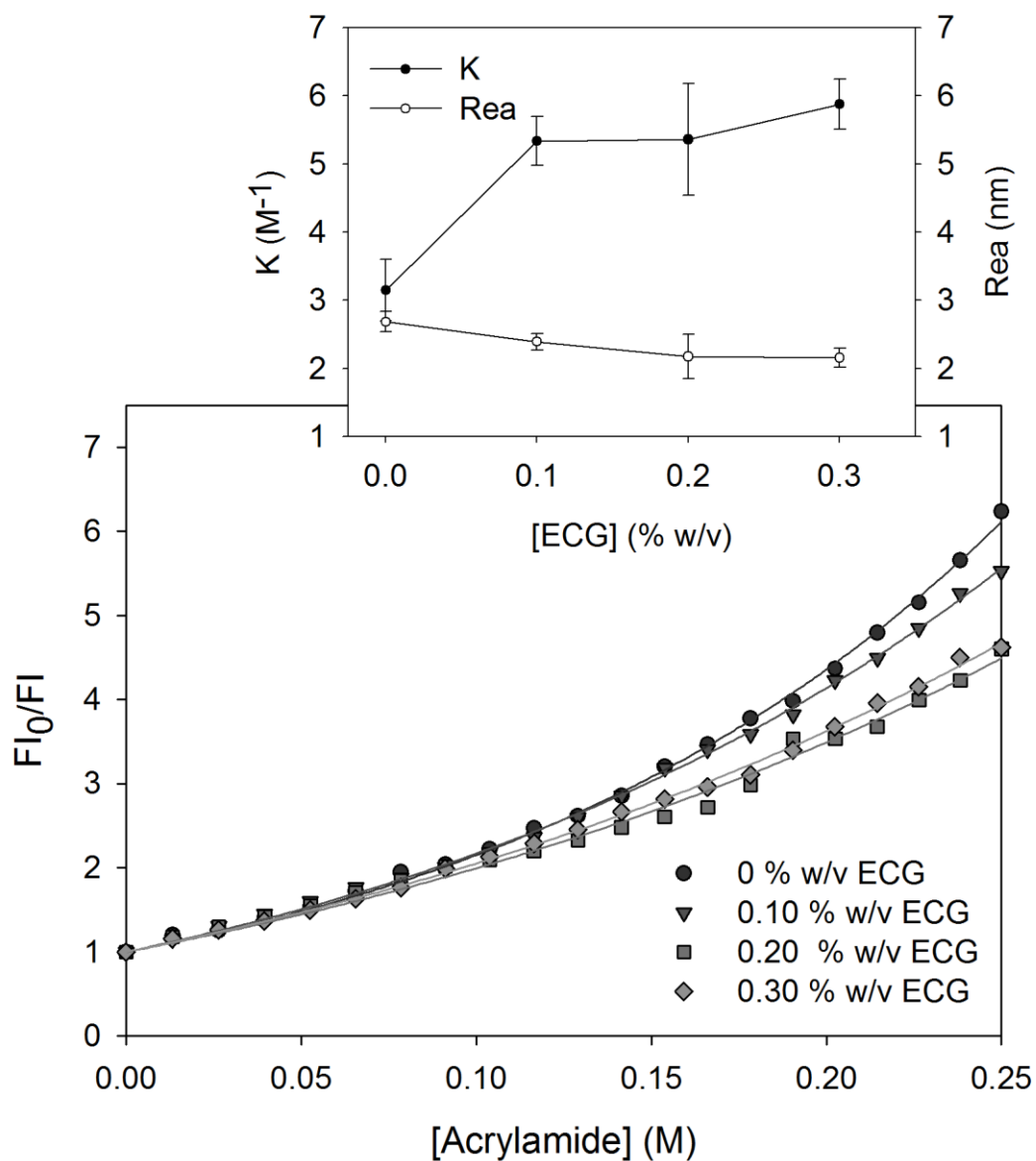
145 Quenching data were presented as Stern-Volmer plots and are shown in Fig. 2. The upward-  
 146 curved resulting plots were interpreted in terms of a modified Stern-Volmer equation, the “sphere  
 147 of action” model, in which the probability of effective quenching in a sphere of volume  $v$ , is unity.  
 148 This situation is described by:

149 
$$FI_0/FI = (1 + KD * [Q]) * \exp^{([Q]*v*N/1000)} \text{ (Eq. 1)}$$

150 where  $v$  is the volume of the sphere,  $N$  is the Avogadro number,  $[Q]$  is the quencher concentration  
 151 and  $KD$  is the dynamic extinction constant (Lakowicz, 2007). Therefore, the Stern-Volmer curves  
 152 obtained were fitted using Equation 1 in order to obtain the sphere radius ( $Rea$ ) and the  $KD$



153 parameter. The KD value represents the reciprocal value of the quencher concentration necessary  
 154 to obtain half of the initial fluorescence of the fluorophores, and Rea represents the average distance  
 155 between the fluorophore and the quencher necessary to assure effective quenching.



156  
 157 Fig. 2: Quenching of intrinsic fluorescence of NaCAS (0.01 % w/v) in the presence of ECG (0-0.3  
 158 % w/v)

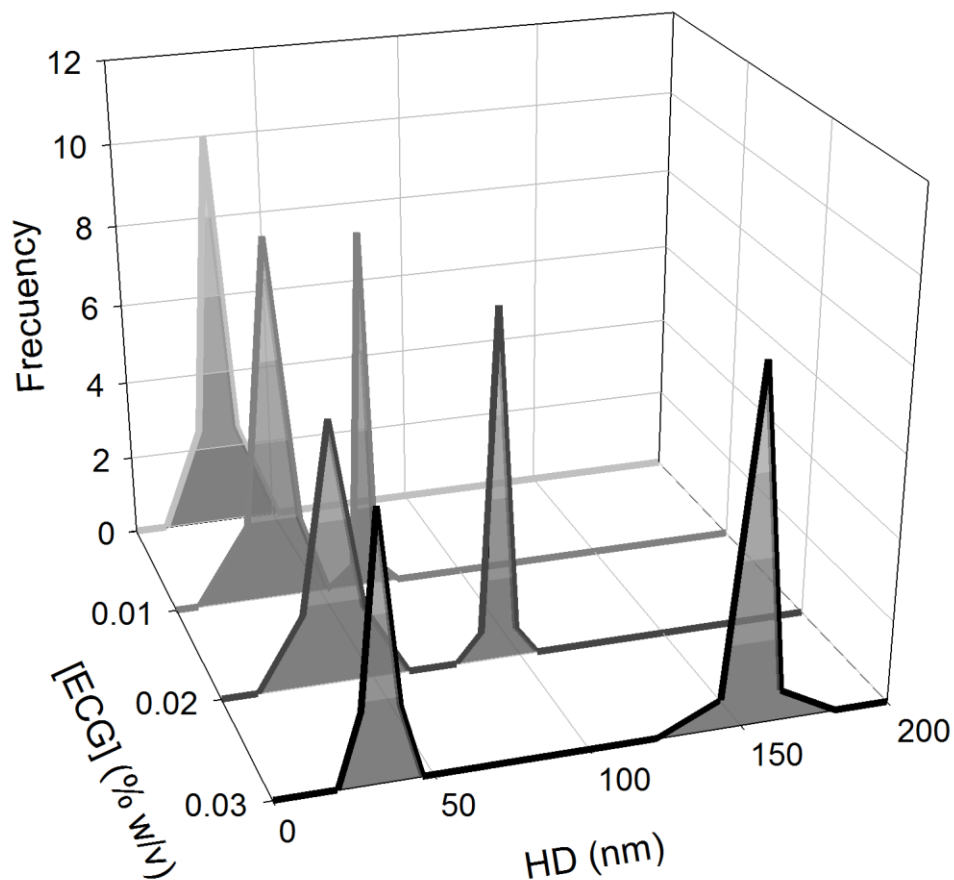
159           The presence of ECG did not affect Rea value ( $p=0.0571$ ). On the other hand, KD increased  
160 from  $3.1 \pm 0.4 \text{ M}^{-1}$  to  $5.5 \pm 0.3 \text{ M}^{-1}$  in the presence of ECG, with no differences among the different  
161 concentrations studied ( $p=0.2542$ ).

### 162 **3.1.3. Surface hydrophobicity**

163           An increase of  $20 \pm 2 \%$  in the  $S_0$  of NaCAS particles was found in the presence of ECG.  
164 There was no statistical difference between the effects of the different ECG concentrations studied  
165 ( $p=0.333$ ).

### 166 **3.2. Determination of hydrodynamic diameter and zeta-potential**

167           The hydrodynamic diameter (HD) distributions of NaCAS aggregates in the presence of  
168 increasing concentrations of ECG are shown in Fig. 3. All samples showed a submicellar form  
169 whose size averaged 20 nm, in agreement with the studies reported by Chu et al. (1995). In the  
170 presence of ECG, another population with a higher HD was found. Its HD increased with increasing  
171 the concentration of the polysaccharide.



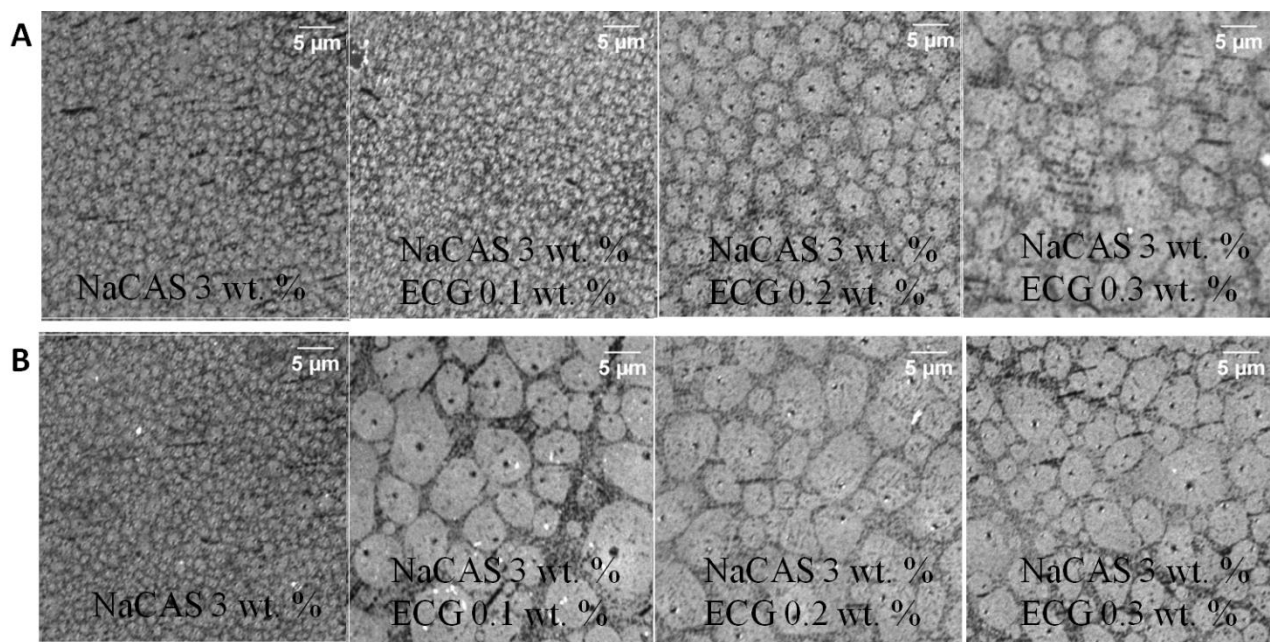
172  
 173 Fig. 3: Hydrodynamic diameter distributions of NaCAS aggregates (0.01 % w/v) in the presence  
 174 of increasing concentrations of ECG (0- 0.03 % w/v).

175 Zeta potential of NaCAS was  $-10.5 \pm 0.7$  mV and it was not affected by the presence of the  
 176 ECG concentrations studied ( $p=0.6786$ ).

### 177 3.3. Visualization of the NaCAS/ECG mixed systems by CSLM

178 The effect of the presence of ECG on 3 % NaCAS dispersions was visualized by CSLM.  
 179 Fig. 4 shows the images obtained for NaCAS and NaCAS/ECG mixtures. Protein appears as bright  
 180 areas due to Rhodamine labeling, while the aqueous phase corresponds to dark regions.

181 As seen from the images obtained, the distribution of NaCAS particles (in the absence of  
182 ECG) did not change throughout the 24-h incubation at 35 °C. On the other hand, when ECG was  
183 added to the systems, an increase in the particle size of NaCAS was observed when the systems  
184 were visualized after mixing. This was more evident at higher ECG concentrations. In addition, the  
185 systems visualized after 24-hour incubation showed the presence of protein aggregates larger than  
186 those observed prior to incubation. All the ECG concentrations assayed led to NaCAS aggregates  
187 of similar size after 24-h incubation.



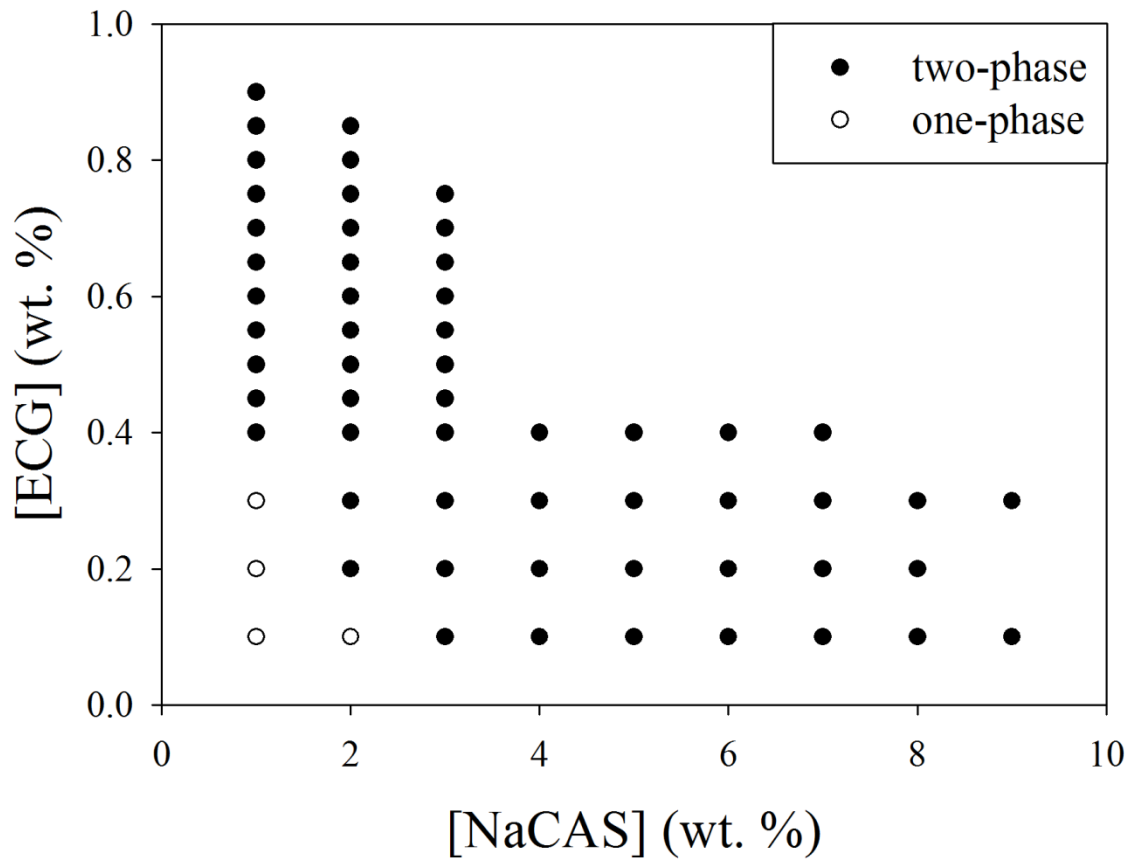
188  
189 Fig. 4: Confocal laser scanning microscopy of NaCAS and NaCAS/ECG mixed systems, A) before  
190 and B) after 24-h incubation at 35 °C. The scale bar attached to the images represents 5 μm.

191

### 192 3.4. Evaluation of the biopolymer concentration ranges for phase separation

193 In order to determine the phase diagram of NaCAS/ECG, several systems composed by  
194 different concentrations of NaCAS (up to 9% every 1%) and ECG (up to 0.9%) were prepared and  
195 incubated at 35°C for 24 h. Fig. 5 shows that there is only one homogeneous phase in the systems

196 containing low biopolymer concentrations (up to ~2% NaCAS and up to ~0.3% ECG), and that  
197 there are two liquid phases in the systems containing higher biopolymer concentrations.  
198 (Tolstoguzov, 2004).



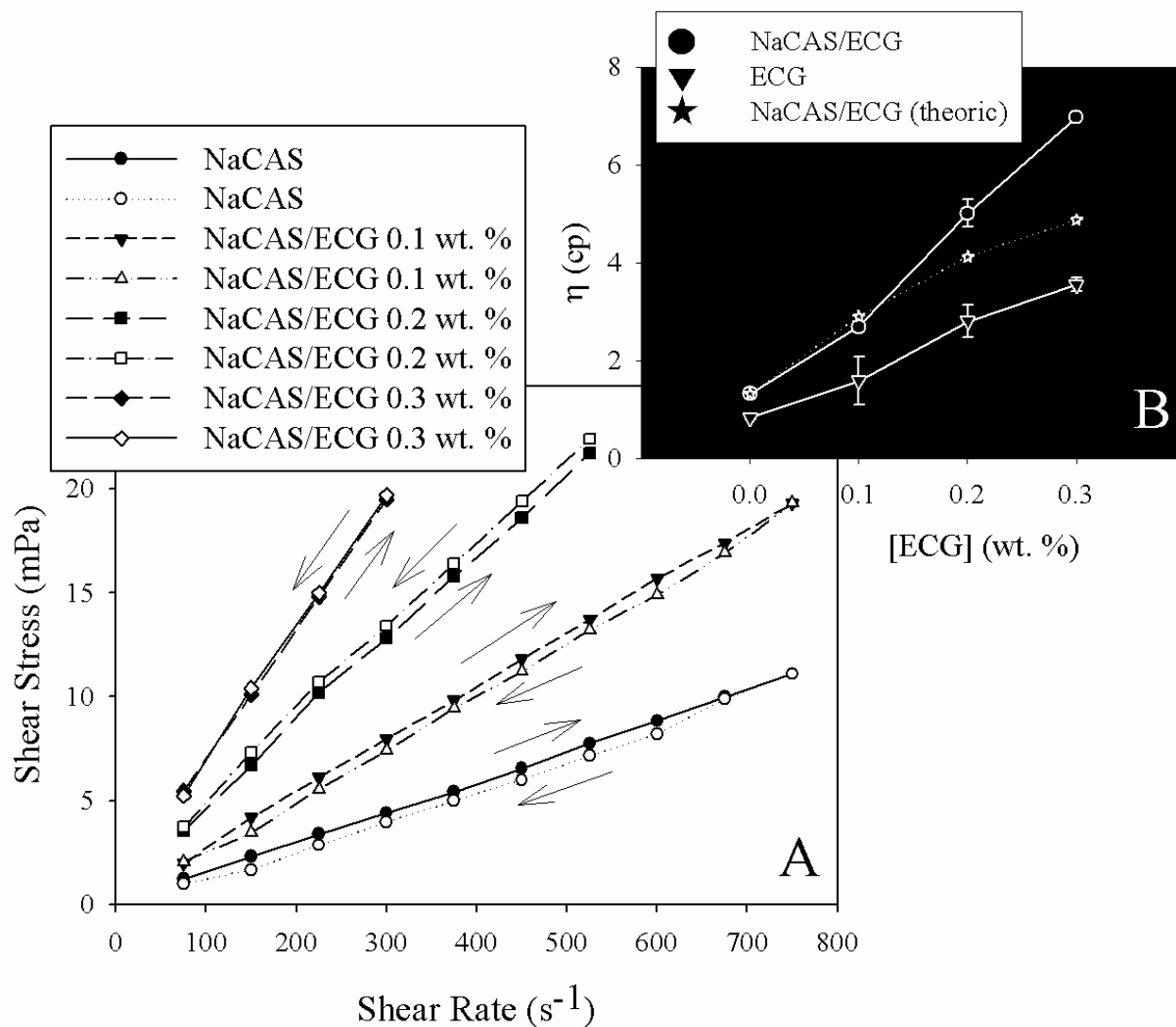
199  
200 Fig. 5: Phase separation of NaCAS/ECG mixed systems. Incubation: 24 h at 35 °C. (Black dots  
201 represent systems which exhibited phase separation whereas white dots represent one-phase  
202 systems).

203

### 204 3.5. Viscosity

205 Fig. 6 shows the flow curves displayed by NaCAS and NaCAS/ECG solutions (immediately  
206 after mixing) and the apparent viscosity ( $\eta$ ) values for NaCAS, NaCAS/ECG and ECG systems at  
207 a fixed shear rate of  $75\text{s}^{-1}$ .

208 NaCAS solutions with and without the addition of ECG exhibited Newtonian behaviour at  
209 the range of shear rate tested, with no significant differences between the flow curves before and  
210 after shearing and resting. Our results also show that viscosity increased as ECG concentration  
211 increased. Moreover, a synergistic effect was observed, since the  $\eta$  of the NaCAS/ECG mixture  
212 was higher than the arithmetic sum of the  $\eta$  of NaCAS and ECG at each concentration (inset Fig.  
213 6).



214  
 215 Fig. 6: Effect of ECG (0-0.3 wt. %) on the flow behaviour of NaCAS systems (3 wt. %).  
 216 Temperature: 35 °C. Inset) Effect of ECG (0-0.3 wt. %) on the viscosity of NaCAS systems (3 wt.  
 217 %). In addition, the predicted viscosity value for the NaCAS/ECG mixtures was represented. This  
 218 value was obtained from the sum of the viscosity values of NACAS and ECG in aqueous systems.  
 219

## 220 4. Discussion

### 221 4.1. Spectroscopic studies of NaCAS/ECG diluted mixed systems

#### 222 4.1.1. Intrinsic fluorescence spectra

223 As pointed out in Section 3.1.1, there was an increase in FI. However, as NaCAS lacks a  
224 defined tertiary structure (Marinova et al., 2009), the increase in FI values could not be clearly  
225 related to a change in the environment of the intrinsic protein fluorophores. Therefore, other factors  
226 must be responsible for this behaviour. The changes observed in the emission spectra would be  
227 associated to the fact that ECG raised the viscosity of the media (Perduca et al., 2013) so that  
228 relaxation process (non-radiant) may be disfavoured.

#### 229 **4.1.2. Quenching of the intrinsic fluorescence**

230 Since the Rea values did not change in the presence of ECG, this may suggest that the  
231 protein intrinsic fluorophore, i.e. the Trp residues of NaCAS, and the quencher (acrylamide),  
232 proved to be at the same distance with and without the addition of ECG. On the other hand, the  
233 effect of ECG on the KD values means that a lower concentration of acrylamide was required to  
234 produce the same quenching effect when ECG was present. This may indicate that the presence of  
235 ECG produces a higher interaction between the fluorophores in the protein and the water  
236 molecules, probably due to a preferential exclusion of ECG from the protein surface.

#### 237 **4.1.3. Surface hydrophobicity**

238 The increase in the  $S_0$  of NaCAS when ECG was added suggests a higher exposition of  
239 hydrophobic residues to the surface, so that ANS/NaCAS interaction was favoured when ECG is  
240 present. Cheng et al. (2015) reported that if the  $S_0$  of a milk protein suspension increased in the  
241 presence of a polysaccharide, it could suggest that these biopolymers do not interact effectively.  
242 This is in agreement with previous results that indicate that ECG is excluded from the protein  
243 surface. Hence, ECG would be likely to favour the aggregation of NaCAS.

#### 244 **4.2. Hydrodynamic diameter and zeta potential**

245 These results suggest that the presence of ECG may induce the formation of NaCAS  
246 aggregates, whose sizes depend on ECG concentration.



247 Since electrostatic repulsion is one of the stabilization mechanisms of NaCAS aggregates  
248 in solution (Horne, 2002; Partanen et al., 2008), it is important to determine the effect of the ECG  
249 on the protein surface charge distribution. Zeta potential of NaCAS was not affected by the  
250 presence of the ECG concentrations studied, suggesting that there was no modification in the  
251 surface charge of the NaCAS particles in the presence of ECG. These results confirm that even if  
252 ECG favours NaCAS aggregation, charge density distribution on the protein surface is not  
253 modified.

#### 254 **4.3. Visualization of the NaCAS/ECG mixed systems by CSLM**

255 The increase in the particle size of the NaCAS due to the addition of ECG suggests that the  
256 presence of ECG favours NaCAS self-aggregation. Moreover, the increase in the size of the protein  
257 particles after 24-hour incubation suggests that ECG affects not only the aggregation of NaCAS  
258 but also the stability of NaCAS in solution (Sharafbafi, Alexander, Tosh, & Corredig, 2015). These  
259 results obtained for concentrated systems are in agreement with those obtained for diluted systems,  
260 discussed in Section 4.2.

261 As several systems composed of galactomannans and caseins were known to phase-separate  
262 (Antonov, Lefebvre, & Doublier, 1999; Kasapis, 1995; Neiryck, Dewettinck, & Van Der Meeren,  
263 2007), it is important to determine the biopolymer concentrations which produce phase separation.

#### 264 **4.4. Evaluation of the biopolymer concentration ranges for phase separation**

265 A relatively low concentration of ECG is needed to induce phase separation in NaCAS  
266 systems. However, even lower concentrations of guar gum were needed to induce phase separation  
267 in NaCAS/guar gum mixtures (Hidalgo et al., 2015). The excluded volume effect is often  
268 considered to be responsible for segregative phase separation in polymer mixtures (Samy Gaaloul,  
269 2010). The differential effects of ECG and guar gum on phase separation can be explained by  
270 taking into account that ECG showed lower molecular weight than guar gum (Perduca et al., 2013).

271 In agreement with this, Bourriot et al. (1999) had reported that a low molecular weight hydrocolloid  
272 induces a lesser extent of exclusion from the protein surface. Thus, the phase separation of  
273 NaCAS/ECG mixtures occurred at higher biopolymer concentrations than those in NaCAS/guar  
274 gum systems.

275 In two-phase systems, a clear difference between the lower and upper phase could be  
276 distinguished: a clear upper phase and a relatively opaque lower phase were formed after  
277 separation. The concentrations of NaCAS and ECG were determined in each phase in order to  
278 determine the critical point, the tie lines and the binodal curve. The lower phase was enriched in  
279 NaCAS and the upper one in the polysaccharide. This result was also seen in different biopolymer  
280 mixtures, where the upper phase was mostly enriched in the galactomanann (Hidalgo et al., 2015;  
281 Perrechil et al., 2009). This phenomenon is caused by the different density of each biopolymer  
282 phase. However, it was not possible to determine the equilibrium concentrations of these two  
283 biopolymers in each phase since the composition and the volume of each phase varied with  
284 incubation time (from 24 h to 72 h).

285 Biopolymer mixtures are known to phase-separate segregatively due to two possible  
286 mechanisms: either to depletion flocculation or to thermodynamic incompatibility (Goh, Sarkar, &  
287 Singh, 2008). The main difference between these phenomena is that the former is of a non-  
288 equilibrium nature (Parris, Kato, Creamer, & Pearce, 1996). According to our results, depletion  
289 flocculation takes place in NaCAS/ECG mixed systems.

#### 290 **4.5. Viscosity**

291 The synergism observed between ECG and NaCAS regarding the viscosity of the systems  
292 could be due to changes in the NaCAS structure in solution as a result of the presence of ECG.  
293 Comparing our results with those obtained by Bourriot et al. (1999) in guar gum/casein micelles

294 systems, it could be concluded that the flocculation of NaCAS as a result of the exclusion of the  
295 EGC from the protein surface is responsible for the behaviour observed.

## 296 **5. Conclusion**

297 In this work we propose that EGC addition causes NaCAS aggregation through depletion  
298 flocculation, since the galactomannan is excluded from the NaCAS surface. A better understanding  
299 of these mixed systems could lead to the development of improved food formulations.

## 300 **Acknowledgements**

301 This work was supported by grants from the Fundación Nuevo Banco de Santa Fe,  
302 Universidad Nacional de Rosario (UNR), 1BIO358 and 1BIO385, from Consejo Nacional de  
303 Investigaciones Científicas y Técnicas (CONICET, Argentina) (PIP 2014-2016 GI) and from  
304 FONCyT (PICT 2011-1354). The authors would like to thank the English Area of Facultad de  
305 Ciencias Bioquímicas y Farmacéuticas, UNR, for manuscript revision. Débora N. López and  
306 Micaela Galante are research awardees of CONICET, Argentina.

307

308 **References**

- 309 Albuquerque, P. B., Barros, W., Santos, G. R., Correia, M. T., Mourão, P. A., Teixeira, J. A. (2014).  
310 Characterization and rheological study of the galactomannan extracted from seeds of *Cassia*  
311 *grandis*. *Carbohydrate polymers*, *104*, 127-134.
- 312 Anema, S. G., & Klostermeyer, H. (1996).  $\zeta$ -Potentials of casein micelles from reconstituted skim  
313 milk heated at 120 C. *International Dairy Journal*, *6*, 673-687.
- 314 Antonov, Y. A., Lefebvre, J., & Doublier, J. L. (1999). On the one-phase state of aqueous protein-  
315 uncharged polymer systems: Casein-guar gum system. *Journal of Applied Polymer Science*,  
316 *71*, 471-482.
- 317 Balaghi, S., Mohammadifar, M. A., & Zargaraan, A. (2010). Physicochemical and Rheological  
318 Characterization of Gum Tragacanth Exudates from Six Species of Iranian *Astragalus*.  
319 *Food Biophysics*, *5*, 59-71.
- 320 Bourriot, S., Garnier, C., & Doublier, J.-L. (1999). Phase separation, rheology and microstructure  
321 of micellar casein-guar gum mixtures. *Food Hydrocolloids*, *13*, 43-49.
- 322 Cerezo, A. S. (1965). The Constitution of a Galactomannan from the Seed of *Gleditsia*  
323 *amorphoides*. *The Journal of Organic Chemistry*, *30*, 924-927.
- 324 Cheng, J., Ma, Y., Li, X., Yan, T., & Cui, J. (2015). Effects of milk protein-polysaccharide  
325 interactions on the stability of ice cream mix model systems. *Food Hydrocolloids*, *45*, 327-  
326 336.
- 327 Chu, B., Zhou, Z., Wu, G., & Farrell, H. M. (1995). Laser light scattering of model casein solutions:  
328 effects of high temperature. *Journal of Colloid and Interface Science*, *170*, 102-112.
- 329 Dickinson, E. (1989). Food colloids — An overview. *Colloids and Surfaces*, *42*, 191-204.
- 330 Dickinson, E. (1998). Stability and rheological implications of electrostatic milk protein-  
331 polysaccharide interactions. *Trends in Food Science & Technology*, *9*, 347-354.

332 Gaucheron, F., Le Graet, Y., Boyaval, E., & Piot, M. (1997). Binding of cations to casein  
333 molecules: importance of physicochemical conditions. *Milchwissenschaft*, 52, 322-327.

334 AOAC. (2008) Milk proteins ((pp. 347-376): Academic Press San Diego, CA.

335 Hidalgo, M. E., Fontana, M., Armendariz, M., Riquelme, B., Wagner, J. R., & Risso, P. (2015).  
336 Acid-Induced Aggregation and Gelation of Sodium Caseinate-Guar Gum Mixtures. *Food*  
337 *Biophysics*, 10, 181-194.

338 Horne, D. S. (2002). Casein structure, self-assembly and gelation. *Current Opinion in Colloid &*  
339 *Interface Science*, 7, 456-461.

340 Kasapis, S. (1995). Review: phase separated, glassy and rubbery states of gellan gum in mixtures  
341 with food biopolymers and co-solutes. *International Journal of Food Science &*  
342 *Technology*, 30, 693-710.

343 Kato, A., & Nakai, S. (1980). Hydrophobicity determined by a fluorescence probe method and its  
344 correlation with surface properties of proteins. *Biochimica et Biophysica Acta (BBA)-*  
345 *Protein Structure*, 624, 13-20.

346 Lakowicz, J. R. (2007). *Principles of fluorescence spectroscopy*: Springer Science & Business  
347 Media.

348 Marinova, K. G., Basheva, E. S., Nenova, B., Temelska, M., Mirarefi, A. Y., Campbell, B. (2009).  
349 Physico-chemical factors controlling the foamability and foam stability of milk proteins:  
350 Sodium caseinate and whey protein concentrates. *Food Hydrocolloids*, 23, 1864-1876.

351 Matignon, A., Moulin, G., Barey, P., Desprairies, M., Mauduit, S., Sieffermann, J. M. (2014).  
352 Starch/carrageenan/milk proteins interactions studied using multiple staining and Confocal  
353 Laser Scanning Microscopy. *Carbohydrate Polymers*, 99, 345-355.

354 Mende, S., Peter, M., Bartels, K., Dong, T., Rohm, H., & Jaros, D. (2013). Concentration dependent  
355 effects of dextran on the physical properties of acid milk gels. *Carbohydrate Polymers*, *98*,  
356 1389-1396.

357 Mohajer, S., Rezaei, M., & Hosseini, S. F. Physico-chemical and microstructural properties of fish  
358 gelatin/agar bio-based blend films. *Carbohydrate Polymers*.

359 Neiryneck, N., Dewettinck, K., & Van Der Meeren, P. (2007). Influence of pH and biopolymer ratio  
360 on sodium caseinate—guar gum interactions in aqueous solutions and in O/W emulsions.  
361 *Food Hydrocolloids*, *21*, 862-869.

362 Parris, N., Kato, A., Creamer, L. K., & Pearce, J. (1996). *Macromolecular Interactions in Food*  
363 *Technology*: ACS Publications.

364 Partanen, R., Autio, K., Myllärinen, P., Lille, M., Buchert, J., & Forssell, P. (2008). Effect of  
365 transglutaminase on structure and syneresis of neutral and acidic sodium caseinate gels.  
366 *International Dairy Journal*, *18*, 414-421.

367 Pavón, Y. L., Lazzaroni, S. M., Sabbag, N. G., & Rozycki, S. D. (2014). Simultaneous effects of  
368 gelatin and espina corona gum on rheological, physical and sensory properties of  
369 cholesterol-reduced probiotic yoghurts. *International Journal of Food Science &*  
370 *Technology*, *49*, 2245-2251.

371 Perduca, M. J., Spotti, M. J., Santiago, L. G., Judis, M. A., Rubiolo, A. C., & Carrara, C. R. (2013).  
372 Rheological characterization of the hydrocolloid from *Gleditsia amorphoides* seeds. *LWT-*  
373 *Food Science and Technology*, *51*, 143-147.

374 Perrechil, F., Braga, A., & Cunha, R. (2009). Interactions between sodium caseinate and LBG in  
375 acidified systems: Rheology and phase behavior. *Food Hydrocolloids*, *23*, 2085-2093.

376 Rosa-Sibakov, N., Hakala, T. K., Sözer, N., Nordlund, E., Poutanen, K., & Aura, A.-M. (2016).  
377 Birch pulp xylan works as a food hydrocolloid in acid milk gels and is fermented slowly in  
378 vitro. *Carbohydrate Polymers*, 154, 305-312.

379 Saha, D., & Bhattacharya, S. (2010). Hydrocolloids as thickening and gelling agents in food: a  
380 critical review. *Journal of food science and technology*, 47, 587-597.

381 Samy Gaaloul, S. L. T., Milena Corredig. (2010). Phase Behavior of Whey Protein Aggregates/ $\kappa$ -  
382 Carrageenan Mixtures: Experiment and Theory. *Food Biophysics*, 5, 103-113.

383 Sharafbafi, N., Alexander, M., Tosh, S. M., & Corredig, M. (2015). Dynamics of Phase Separation  
384 in Oat  $\beta$ -glucan/Milk Mixtures Studied with Ultrasonic and Diffusing Wave Spectroscopy.  
385 *Food Biophysics*, 10, 66-75.

386 Spotti, M. J., Santiago, L. G., Rubiolo, A. C., & Carrara, C. R. (2012). Mechanical and  
387 microstructural properties of milk whey protein/espina corona gum mixed gels. *LWT - Food*  
388 *Science and Technology*, 48, 69-74.

389 Tavares, C., & Da Silva, J. L. (2003). Rheology of galactomannan–whey protein mixed systems.  
390 *International Dairy Journal*, 13, 699-706.

391 Tavares, C., Monteiro, S. R., Moreno, N., & Da Silva, J. L. (2005). Does the branching degree of  
392 galactomannans influence their effect on whey protein gelation? *Colloids and Surfaces A:*  
393 *Physicochemical and Engineering Aspects*, 270, 213-219.

394 Tolstoguzov, V. (2004). Why were polysaccharides necessary? *Origins of Life and Evolution of*  
395 *the Biosphere*, 34, 571-597.

396

397